Evaluation of Interaction Effect of Sulfate and Chloride Ions on Reinforcements in Simulated Marine Environment Using Electrochemical Methods

Lujia Yang[1], Yunze Xu[1], Yesen Zhu[1], Liang Liu[1], Xiaona Wang[2,*], Yi Huang[1]

[1] School of Naval Architecture, Dalian University of Technology, Dalian 116023, China
[2] School of Physics and Optoelectronic Engineering, Dalian University of Technology, Dalian 116023, China
*E-mail: wangxn@dlut.edu.cn

The general corrosion processes of mild steel caused by the introduction of chloride ions and sulfate ions in simulated marine environment were studied by the measurements of open circuit potential (OCP), linear polarization resistance (LPR) and electrochemical impedance spectroscopy (EIS) methods. Moreover, wire beam electrode (WBE) was employed to evaluate the action effects of both sulfate and chloride ions for the propagation of localized corrosion in the simulated pore solution. OCP, LPR and EIS measurement results indicated that in simulated marine environment sulfate ions only had slight influence for the passive film compared to chloride ions which could rapidly destroy the passive film on the steel surface. Meanwhile, sulfate ions could also decrease the corrosion rate of the steel in chloride-induced corrosion process. Furthermore, WBE test results revealed that localized corrosion behavior was mitigated by the introduction of sulfate ions in simulated marine environment.

1. INTRODUCTION

Concrete is one of the most widely consumed construction material in the world. Steel reinforcements in concrete structures are usually passivated by a protective film of γ-ferric oxide layer due to the high alkalinity of the pore solution [1]. Consequently, the corrosion rate of the steel in concrete is always quiet low. However, failures of the steel in various concrete structures such as tunnels, bridges and dams have been detected due to the ingression of pollution ions which are usually introduced by the acid rain or overuse of de-icing salts [2]. In particular, the steel in the concrete structures which are under marine environment may suffer higher corrosion risks due to the high

concentrations of the pollution ions such as chloride ions and sulfate ions in sea water. The passive film on the steel surface will be damaged by the aggressive ions and localized corrosion will initiate on the steel surface [3-7]. Once localized corrosion attacks occur, pits or crevices on the steel surface may propagate rapidly and eventually leads to the failure of the structure [8]. Therefore, it is important to know the effect of aggressive ions in the seawater on the corrosion behavior of the steel reinforcement.

Traditional methods of studying the corrosion behavior of reinforcement include liner polarization resistance (LPR), electrochemical impedance spectroscopy (EIS) and half-cell potential techniques [9-14]. For instance, LPR method has been applied to determine corrosion current density of buried electrode. EIS has also become an effective technique for the evaluation of the steel corrosion and its inhibition in concrete condition based on equivalent circuit analysis. Half-cell potential measurements are always used in the anodic sensor ladder system which can map corrosion potential of the steel embedded in different locations of the concrete structure. Although these electrochemical measurements are useful and having rapid response to the corrosion monitoring of buried steel, they are often hard to perform due to the high electrical resistance of the thick concrete layer on the steel surface. As LPR and EIS can only provide general corrosion information due to their measurement principle, localized corrosion caused by the degradation of the passive film is difficult to be evaluated based on these traditional methods. In recent researches [15-20], the wire beam electrode (WBE) has been applied for the study of localized corrosion behavior in various tests. WBE can simulate the corrosion processes on a simulated one-piece electrode by continuously mapping the potential and galvanic current on the surface of WBE. Because no polarization was applied on the WBE surface, it can be used as an in-situ technique for the monitoring of localized corrosion in concrete structures.

Based on the electrochemical techniques mentioned above, the corrosion behaviors of reinforcement steels caused by chloride and sulfate ions have been studied in considerable tests. In Kasturie's research [21], bare steel coupons were directly immersed into the solution contained with sulfate ions and chloride ions, respectively, without prepassivation. Serious pitting corrosion patterns were observed on the surfaces of the steel coupons exposed to both solutions. It was also found that adding sulfate ions into the chloride ions contained pore solution could further enhance the corrosion rate. Haleem [22] even found that the sulfate ion was more aggressive than the chloride ion through the monitoring of open circuit potential (OCP) in different solution conditions. However, a different result was obtained in the test conducted by Al-Amoudi [23] who mounted a concrete specimen in the solution only contained with sulfate ions. The half-cell potential of the steel in the concrete was still above -200 mV after exposed to the solution for 500 days, indicating sulfate ions have no aggressive effect on passivated film in pore solution. Furthermore, the breakdown of the passive film was delayed over double period in the solution contained with both chloride and sulfate ions compared to that in the solution only contained with chloride ions. The test results were further verified by using different kinds of concretes in the other tests completed by Al-Amoudi [24]. In addition, Al-Tayyib [25] found the same mitigation effect of the sulfate ions on the corrosion behavior of steels in chloride ions contained solution and ascribed it to the re-formation of a sulfate film layer on the steel surface. In recent studies, ion-competitive adsorption of sulfate ions and chloride ions on the metal surface was

found which could further explain the inhibition of pitting corrosion in some conditions with the introduction of sulfate ions [26].

Though plenty of studies were concerned on the corrosion of steels in concrete environment, controversy is still exit on the corrosion processes caused by the pollution ions. The evaluation of the interaction effect of chloride and sulfate ions is rare based on marine environment which contained plenty of aggressive anions. Furthermore, the studies of pollution ions on localized corrosion are also few since only traditional electrochemical methods were used in previous studies. In this work, the individual action effects of sulfate ions and chloride ions with the concentration of seawater on steel corrosion in simulated pore solution were firstly studied by OCP, LPR and EIS measurements. Meanwhile, the interaction effect of the both anions was also tested. Then, the influence of the sulfate ions for localized corrosion in chloride contained solution was further studied by WBE technique.

2. EXPERIMENTAL

2.1 Preparation of the electrodes and simulated pore solutions

The material of the electrodes applied in the test was GB/T700 Q235A carbon steel, with a chemical composition of (wt.%): C 0.22% Si 0.30% Mn 1.40% P 0.045% S 0.05% Cr 0.01% Ni 0.01% and Fe being the balance. The specimens used as the working electrode were machined in a dimension of $10 \times 10 \times 3$ mm^3 (a working surface area of 1.5 cm^2). The specimens were sealed with epoxy resin with the end face exposed to the solution. A copper wire was welded to the back side of the specimen which was sealed in the epoxy. Before each test, the working face was ground sequentially up to 1000 grit silicon carbide paper, rinsed with deionized water and degreased in acetone. In order to prevent crevice corrosion, the edge between the specimens and the epoxy was coated with a masking lacquer before the tests.

The simulated pore solution was the supernatant liquid of the saturated $Ca(OH)_2$ solution with its pH higher than 12.5 which was measured by YSI Proplus pH measurement device. Then the pure saturated $Ca(OH)_2$ solution was divided into four parts and different kinds of chemical reagent was introduced into the solution as below:

Solution 1- pure saturated $Ca(OH)_2$;
Solution 2- Solution 1+ 3% NaCl by weight;
Solution 3- Solution 1+ 0.5% Na_2SO_4 by weight;
Solution 4- Solution 1+ 3% NaCl +0.5% Na_2SO_4 by weight

As it has been investigated that the composition of the sulfate ions is nearly 0.27% in East China Sea, 0.5% Na_2SO_4 was used in this work to simulate the practice sulfate ion concentration at marine environment.

During each test, the simulated pore solution was placed in an air-conditioned room with its temperature kept at 20 ± 2℃. Air sparging of the solution was continued, and the dissolved oxygen (DO) concentration was higher than 5 mg/L which was monitored by YSI Pro ODO monitor.

2.2 Electrochemical measurements

Four sets of three-electrode electrochemical cells separately contained Solution 1 to 4 were used for the OCP, LPR and EIS measurements as shown in Fig. 1. Each three-electrode cell was constructed with the Q235A electrode as working electrode (WE), a platinum plate as counter electrode and a saturated calomel electrode (SCE) as reference electrode (RE). Before the tests, the working electrodes were firstly immersed into Solution 1 over 48 h for prepassivation. Then the four electrodes were transferred to the four cells which contained different kinds of solutions for 30 days electrochemical tests.

During the 30 days immersion period, OCP of each electrode was recorded by connecting to a voltage in CorroTest CS 350 electrochemical workstation and compared with SCE. Electrochemical experiments were also conducted by CS 350 electrochemical workstation. LPR measurements were performed by applying anodic voltages scan at the rate of 0.1 mV/s over a range of ±20 mV around the OCP. EIS test was carried out on steady-state OCP disturbed with amplitude of 10 mV ac sine wave. The frequency ranges were adjusted from 100 KHz to 10 mHz. The four separated three-electrode test systems were alternately connected to the CS 350 workstation through the CS 16X multi-channel auto switch which is also plotted in Fig. 1.
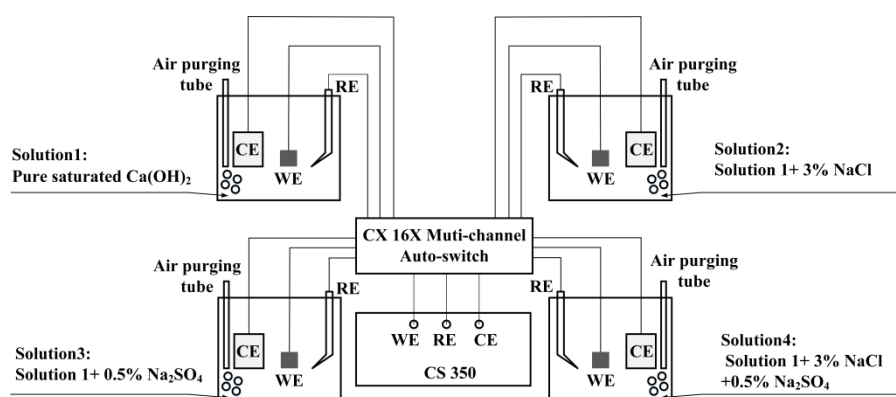

Figure 1. Schematic diagram of electrochemical test cells used for OCP, LPR and EIS measurements

After the electrochemical tests, the four working electrodes were taken out and the corrosion morphologies of the electrodes were observed by FEI Quanta 450 scanning electron microscope (SEM).

2.3 Preparation of WBE and current scanning

A WBE was fabricated of 100 identical wire electrodes (1.5 mm diameter) with a total working area of 1.77 cm^2 as shown in Fig. 2. The materials of the wire electrodes were also made of Q235A steel which were same as the steel electrodes. All the wires were embedded in epoxy resin and

insulated from each other with a very thin epoxy layer. The working surface of WBE was pretreated as same procedures as the electrodes described above.

Fig.2 also shows a schematic experimental setup to monitor the localized corrosion behavior of the steel using a WBE corrosive detection instrument (CST520, Corrtest). In the WBE corrosive detection instrument, there is a 10×10 array autoswitch circuit controlled by a microcomputer to measure the galvanic current. In particular, the current distribution was mapped by measuring the galvanic current between the chosen electrode (W_1) and the other interconnected electrodes (W_2) on the WBE via a multi range zero resistance ammeter (ZRA). During the non-test period, the 10×10 array auto switch circuit was controlled to be electrical connected to simulate electrochemically a conventional one-piece electrode.
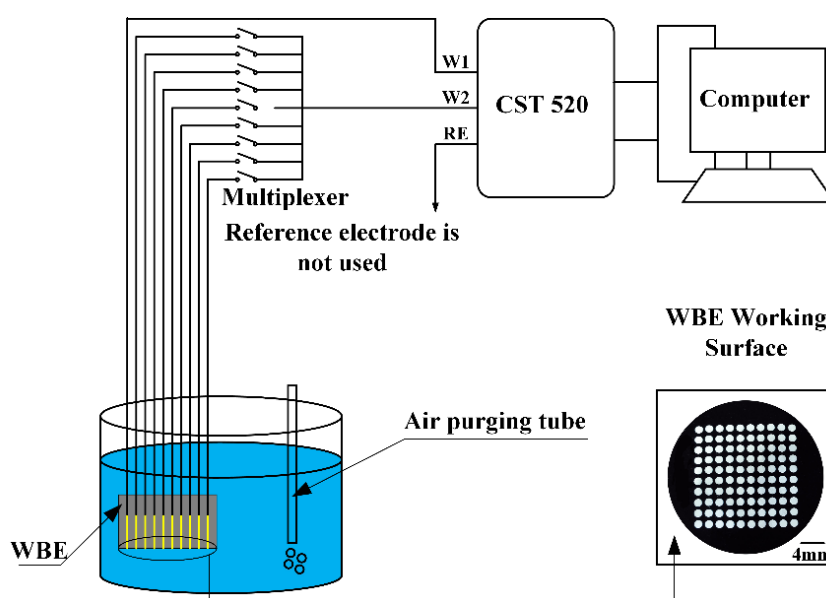

Figure 2. The photo of the WBE surface and the schematic diagram of its current scanning

The solutions used for WBE test were also kept in an air-conditioned room with its temperature kept at $20\pm2\,^{\circ}\mathrm{C}$. The WBE surface was firstly exposed to the pure $Ca(OH)_2$ solution over 48 h for passivation. Then, it was immersed into Solution 2 for a 10 days test. After the first experiment, the WBE was taken out and re-polished. Later, the WBE was put into pure $Ca(OH)_2$ solution again for a 48 h prepassivation. Following, another 10 days test was conducted with the WBE immersed into the solution 4. The DO concentration and pH value were also measured through the test period and kept at the same conditions as that in the electrochemical tests. During each test period, galvanic current information was continually recorded and the current distribution maps were plotted by Origin 8.5. The action effect of sulfate ions for the localized corrosion behavior of WBE in chloride contained pore solution was further analyzed by the calculated parameters obtained from the current distribution maps.

3. RESULTS

3.1 OCP measurement results of the electrodes in Solution 1 to 4

Fig. 3 shows the OCP of the electrodes immersed in different solution conditions. It is seen that the OCP of the electrode in solution 1 only had a slight decrease which may be caused by the dissolve of carbon dioxide in the air leading to a little decrease of pH of the solution. The OCP of the other electrodes all had different degrees of obvious reductions after transferred into Solution 2 to 4. It can be clearly found that the OCP of the electrodes had the largest decrease to -570 mV after exposed to solution 2 for 3 days, indicating the most serious breakdown of the passive film [27]. The OCP of the electrode immersed in Solution 3 decreased to the lowest value of -340 mV in the first 3 days and gradually recovered to a stable value of -250 mV after 10 days. This behavior is attributed to the slightly dissolution of the passive film at first and following formation of a new protective film which is less protective than that of the original iron oxide film. Moreover, it seems that the attack by sulfate ions with the concentration of seawater is less aggressive and dangerous than chloride ions by comparing the OCP of the electrodes in Solution 2 and Solution 3. The OCP of the electrode in the Solution 4 contained both sulfate and chloride ions also had a dramatic decrease in the first 4 days. It is assumed to be due to the oxide film destruction by chloride ions and sulfate ions. Then the potential of the electrode rose to -460 mV after 9 days immersion, it is attributed to the competitive adsorption between sulfate ions and chloride ions, and the reaction on the surface is more similar to that in Solution 2 contained sulfate ions at this period. Eventually, after 30 days test the potential decreased to the value close to -560 mV, which was nearly 50 mV higher than that in Solution 2 suggesting sulfate ions in the seawater might inhibit the chloride-introduced corrosion of the steel.
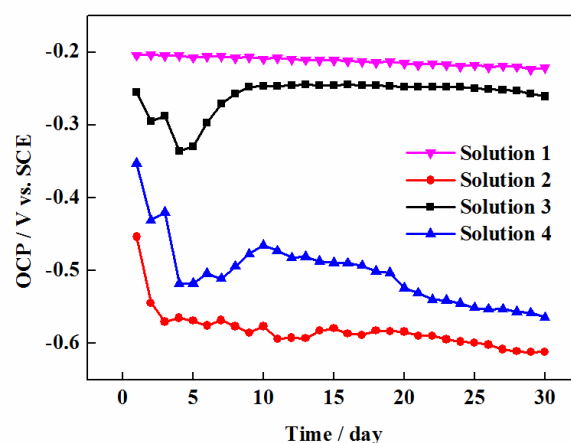

Figure 3. Time dependence of the open circuit potential of the four electrodes immersed in Solution 1 to 4

3.2 LPR measurement results

LPR is widely applied to study the steel corrosion. The corrosion rate of the steel can be calculated by using Stern-Geary equation, which is expressed as:

$$i_{corr} = B / R_p \qquad\qquad (1)$$

Where B is used as a constant value as 26 mV for active corrosion process and 52 mV for passive state, R_p is the polarization resistance which can be calculated from the slopes of the measured liner polarization curves [28]. As it has observed that the OCP of the electrodes in Solution 1 and 3 were always above -300 mV after immersed for over 15 days, it means the status of the both electrodes were passive and B was chosen for 52 mV. While the values of B were used as 26 mV for the other two electrodes exposed to Solution 2 and 4, respectively, due to the significant decreases of the OCP.

Fig. 4 shows the corrosion rates of the electrodes in Solution 1 to 4. The variation of the corrosion rates had same trends with the OCP measurement results. The corrosion rates of the electrodes in Solution 1 were lower than 0.0003 mm/a, suggesting nearly no corrosion occurred on the electrode. While the corrosion rate of the electrode in Solution 2 had the largest increase from 0.014 mm/a to 0.28 mm/a. It indicates chloride ions would cause the dissolution of the passive film on the electrode surface and accelerated the corrosion rate. The maximum corrosion rate of the electrodes in Solution 3 was lower than 0.004 mm/a which is much less than that in Solution 2, indicating that the sulfate ions in the seawater is less corrosive than chloride ions for reinforced steels. It can be clearly found that the corrosion rate of the electrode in Solution 4 was below 0.008 mm/a in the initial period. However, a sudden increase of the corrosion rate was found after the electrode corrosion for 9 days. The significant increase of the corrosion rate from 0.006 mm/a to 0.020 mm/a in Solution 4 was attributed to the thorough breakdown of the passive film on the steel surface which was obtained from OCP results. The corrosion rate of the electrode in Solution 4 was approximately a quarter of that in Solution 2, indicating that the sulfate ions in the seawater could mitigate the aggression of chloride ions.
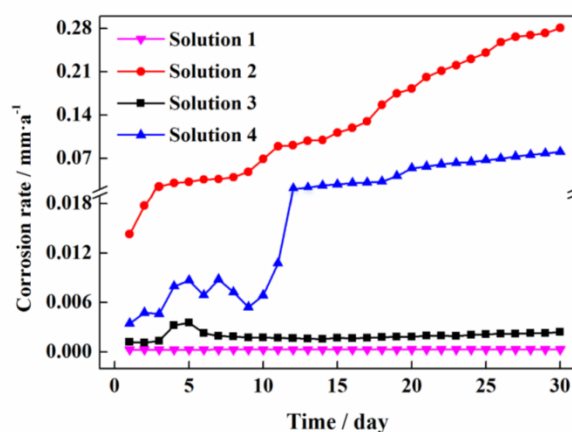

Figure 4. Time dependence of corrosion rates of the electrodes exposed to different solutions

3.3 EIS measurement results

Fig. 5 shows the EIS plots of the electrodes at different immersion time in Solution 1 to 4. It can be seen from Fig. 5a, the electrode in Solution 1 presents a large impedance circle through the whole test period, indicating the passive film on its surface exhibited excellent corrosion resistance.

The electrode in Solution 3 also shows an impedance circle in initial period. However, it can be seen the diameter of the capacitive arc had a rapid decrease at day 4 which is accordance with the OCP and LPR measurement results. The impedance circle recovered in the following period and became stable after corrosion for 11 days. After the electrode immersed in Solution 3 for 30 days, a slight linear tail in low frequency can be observed from Fig. 5c. The linear segment at the low frequency indicates the corrosion process was controlled by the oxygen diffusion process and Warburg impedance should be applied for the represents of oxygen diffusion process for the passive steel in simulated pore solution. More serious corrosion process can be found on the electrode in Solution 2 with the appearance of obvious low frequency tails shown in Fig. 5b. It suggests that chloride ions would soon break the passive film and caused severe corrosion. Same phenomenon was also found in the EIS plots of the electrode in Solution 4. However, the Warburg effect was appeared after the electrode immersed for 11 days, suggesting a long time was needed to damage the passive film with the introduction of sulfate ions into the chloride contained solution.
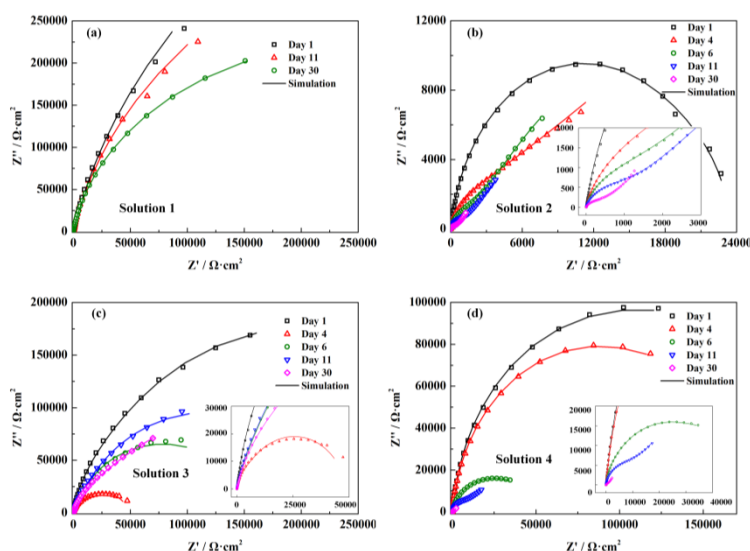

Figure 5. EIS plots of the electrodes immersed for 1, 4, 6, 11 and 30 days in Solution 1 (a) Solution 2 (b) Solution 3 and (c) Solution 4 (d)

3.4 Surface morphologies of the electrodes immersed in Solution 1 to 4

Fig. 6 shows the SEM surface morphologies of the four electrodes immersed in Solution 1 to 4 for 30 days. It is found from Fig. 6a that a dense and thick passive film was on the electrode immersed in Solution 1 and the scratches on the steel surface were clear to be seen. It indicates the electrode in Solution 1 was well protected and nearly no corrosion occurred on its surface. Though the corrosion rate of the electrode in Solution 3 was low in the electrochemical test, tiny pits and slight corrosion patterns could be seen from Fig. 6c. However, a thin protective film and the scratches still could be seen on its surface, suggesting a quiet low corrosion rate in only sulfate ions contained solution. Serious localized corrosion can be seen from Fig. 6b with a large scale of corrosion product. Notice that the corrosion product was porous and expanded to a large area on the steel surface which was

accordance with the corrosion processes in the concrete contained with chloride ions [6]. As shown in Fig. 6d, the surface of the electrode in Solution 4 became rough and pitting and mesa type attacks can be found. However, the corrosion pattern of the electrode in Solution 4 was more close to that shown in Fig. 6c, compared to the serious localized corrosion shown in Fig. 6b. The SEM images show that sulfate ions could inhibit the localized corrosion in chloride contained solution.
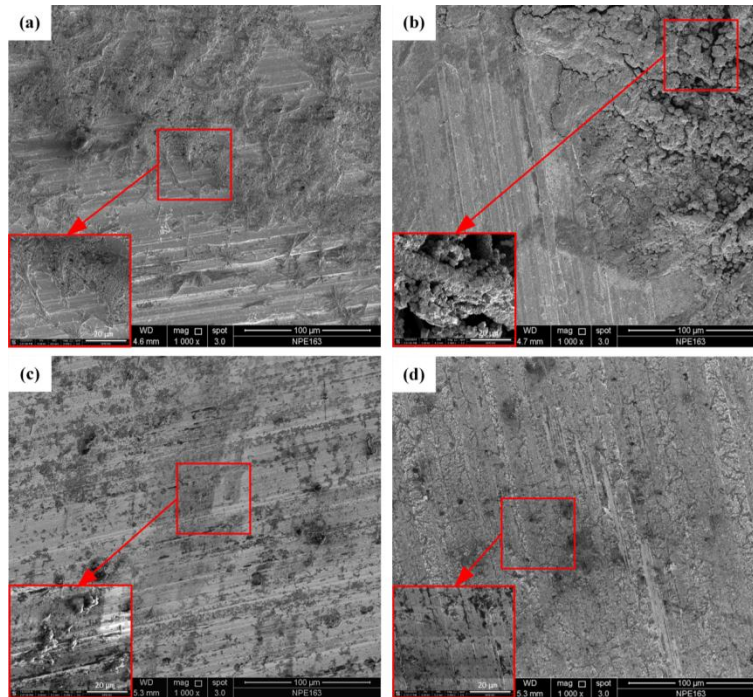

Figure 6. Surface morphologies of the electrodes after corrosion for 30 days in Solution 1 (a) Solution 2 (b) Solution 3 and Solution (4)
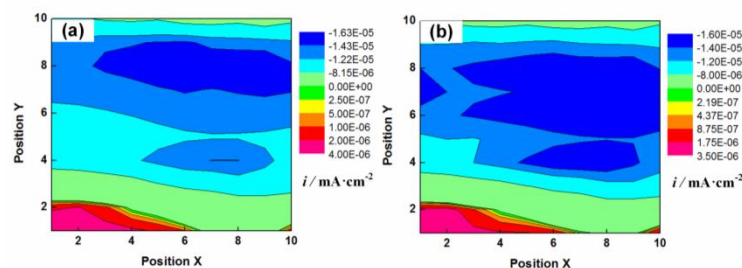
3.5 WBE test results

Figure 7. Galvanic current density distribution maps of the WBE immersed in Solution 1 for 24 h (a) 48 h (b)

To further study the action effect of sulfate ions and chloride ions for localized corrosion behavior, another three groups of 10 days WBE tests were applied for the measurement of galvanic current distribution maps in Solution 2, 3 and 4, respectively. Prior to the test, the WBE were

immersed in Solution 1 for prepassivation for 48 hours. Fig. 7 shows the electrode immersed in Solution 1 for 24 h and 48 h. A large anodic area was found on the WBE surface with a relative small galvanic current density. The anodic area had a slight increase after immersed for 48 h and the current density nearly had no changes, indicating passive film was formed and kept stable on WBE surface.

Fig. 8 shows the galvanic current density distribution maps of the pre-passivated WBE in Solution 2 during different immersion period. It is seen that the distribution of the anodic area on WBE surface were scattered and the anodic galvanic current density had a large increase after transferred into Solution 2 immediately. After 5 days immersion, stable anodic area appeared on the WBE surface with its highest anodic galvanic current density nearly 6000 times higher than that in Solution 1. It indicates pitting corrosion was formed on WBE surface and a stable anodic dissolution rate was kept which can be seen from the slight change of the anodic galvanic current density shown in Fig. 8d after corrosion for 10 days.

Fig. 9 shows the anodic current density of the WBE immersed in Solution 3 for a 10 days test. The anodic current density was much smaller than that in Solution 2 during the whole test. And the anodic area was more stable than that in Solution 2. It suggests only slight uniform corrosion occurred on the WBE surface immersed in Solution 2.

As shown in Fig. 10, the anodic current density of the WBE also had an immediate increase after immersed in Solution 4. The increased amplitude of the anodic current density was 6.5 times smaller than that in Solution 2 after the first day immersion.
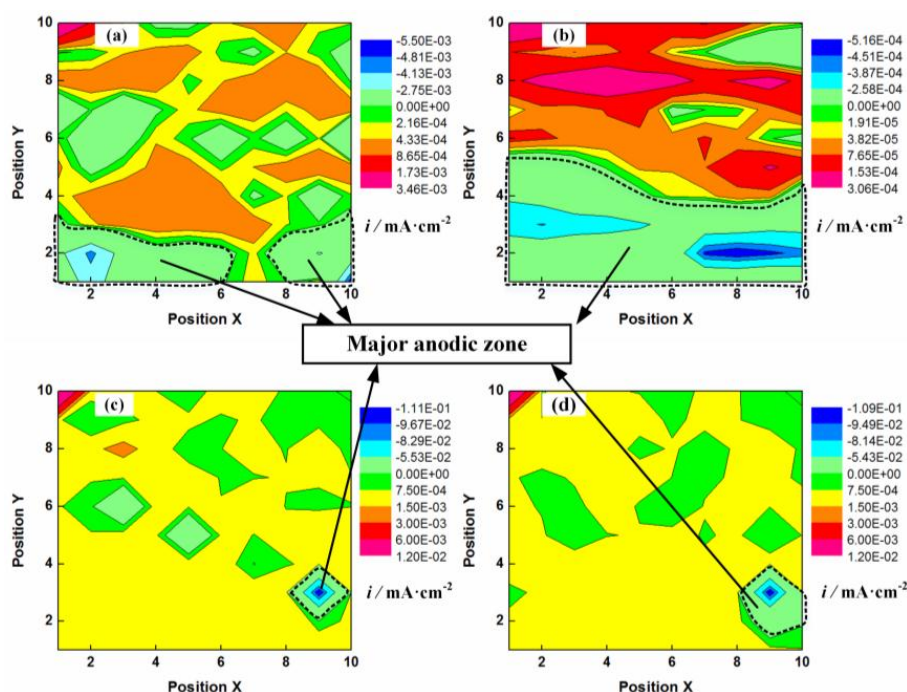

Figure 8. Galvanic current density distribution maps of the WBE immersed in Solution 2 for 1 day (a) 2 days (b) 5 days and 10 days (d)

The anodic current density soon decreased in the following period and had a slight increase after 10 days immersion. The anodic area on the WBE surface was always stable and only had a little

increase through the whole test. It can be found that the anodic sites were concentrated on the WBE surface in only chloride contained solution and serious localized corrosion occurred in these sites. While a quiet larger anodic area was remained on the WBE surface in the solution contained both sulfate and chloride ions with a lower anodic galvanic current density. It suggests the corrosion in Solution 4 tended to average corrosion compared with that in Solution 2. Moreover, the form of the maps in solution 4 was closer to that in Solution 3, indicating that the corrosion form of the WBE in Solution 4 was more similar to that in Solution 3 than that in Solution 2.
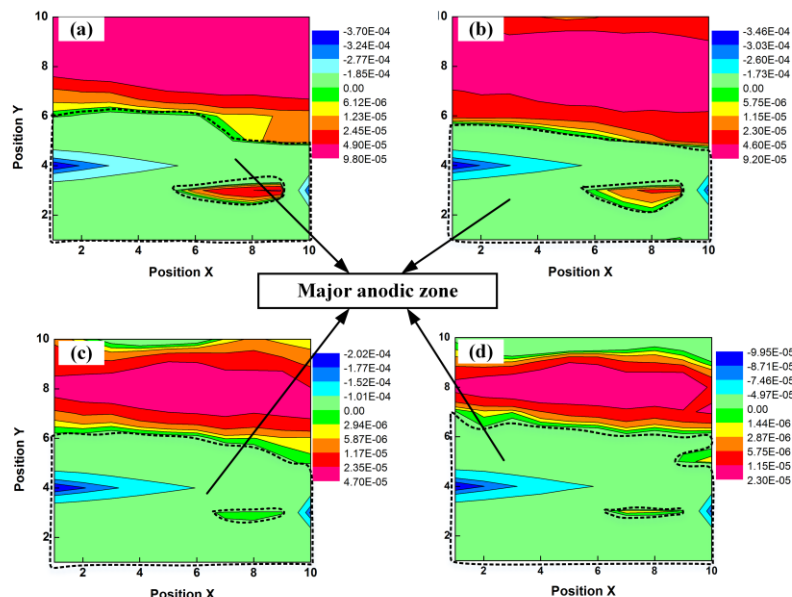

Figure 9. Galvanic current density distribution maps of the WBE immersed in Solution 3 for 1 day (a) 2 days (b) 5 days and 10 days (d)
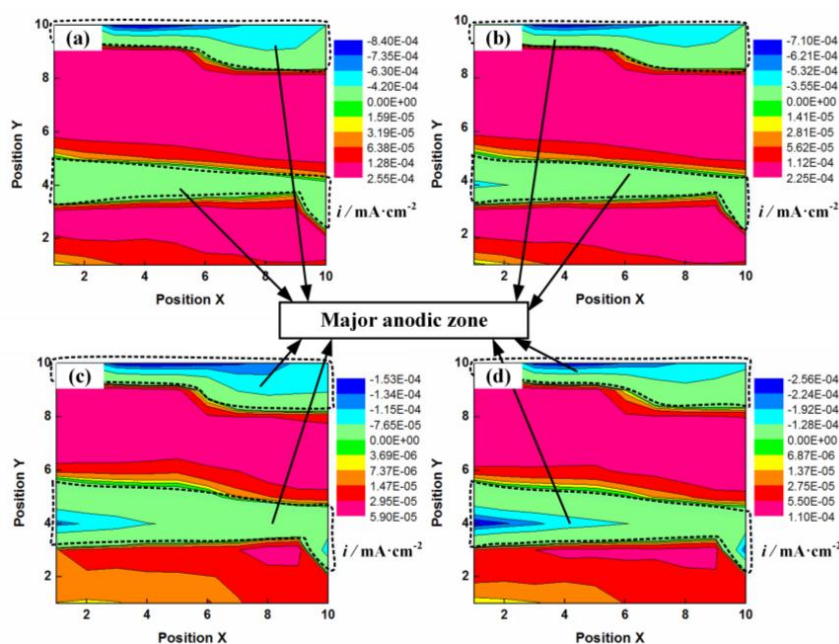

Figure 10. Galvanic current density distribution maps of the WBE immersed in Solution 4 for 1 day (a) 2 days (b) 5 days and 10 days (d)

Fig. 11 shows the changes of the maximum anodic galvanic current density and the total anodic current of WBE after transferred to Solution 2, 3 and 4, respectively. The maximum anodic current density of the WBE in Solution 3 was below 6.63×10^{-5} mA/cm^2 at the end of the test. The maximum corrosion rate of the electrode caused by the galvanic effect can be calculated through the Faraday law [29]:

$$v = Mi_g / nF\rho \qquad (2)$$

Where v is the corrosion rate caused by the galvanic current, i_g is the galvanic current density, n is valence, F is the Faraday constant and ρ is the density of the metal [30].
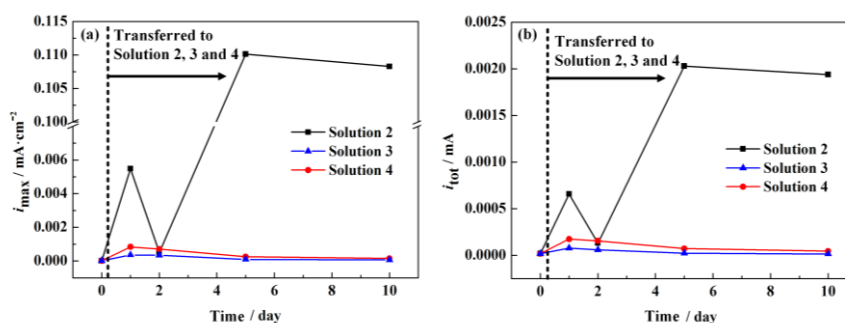

Figure 11. The changes of the maximum anodic galvanic current density (a) and total anodic current (b) after WBE transferred to Solution 2, 3 and 4

The maximum corrosion rate was near 7.8×10^{-4} mm/a which was much smaller than the average corrosion rate measured by LPR, indicating nearly no localized corrosion occurred on WBE surface after immersion in Solution 3 for 10 days. The maximum anodic current density of the electrode in Solution 4 was below 1.53×10^{-4} mA/cm^2 which was higher than that in Solution 3, indicating that the corrosion rate increased by adding chloride ions in the sulfate ions contained pore solution. The maximum corrosion rate of the WBE in Solution 4 was near 1.8×10^{-3} mm/a which was much smaller than the average corrosion rate measured by LPR, indicating nearly no localized corrosion occurred on WBE surface after immersion in Solution 4 for 10 days. The total anodic current of the WBE in Solution 2 had an increase in the initial period of immersion and soon came back with the increase of the anodic area shown in Fig. 11 after corrosion for 10 days. The maximum galvanic current density had a dramatic increase to 0.11 mA/cm^2 after the WBE exposed to Solution 2 for 5 days. It suggests the maximum corrosion rate on WBE surface was 1.3 mm/a which was great larger than the average corrosion rate measured by LPR in Solution 2 [31]. The total anodic current of the WBE in Solution 2 had the same trend with the maximum anodic current density, also indicating localized corrosion behavior on the steel surface.

4. DISCUSSIONS

In the oxygen contained pure saturated calcium hydroxide solution, the anodic dissolution of the electrode will produce FeOOH according to Eqs. (4) and (5) [32]:

$$Fe \rightarrow Fe^{2+} + 2e^{-} \qquad\qquad (3)$$
$$2Fe^{2+} + 1/2O_2(g) + H_2O(l) \rightarrow 2FeOOH(s) + 4e^{-} \qquad\qquad (4)$$
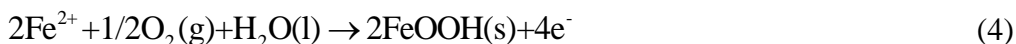
The Q235A steel is passivated by the forming of dense oxidation film on its surface. After the electrodes transferred to the solution contained with aggressive ions, FeOOH will be reduced into Fe_3O_4 or Fe_2O_3 which is less protective. The reduction of the FeOOH will cause the breakdown of the passive film and lead to the initial of pitting corrosion process. Once a pit is initiated on the steel surface, the aggressive ions will soon come into the occluded site and cause continues corrosion due to the self-sustaining effect [33]. The chloride ion is a kind of aggressive ion which leads to a drastic reduction in the stability of the passive film [34]. When part of the passive film is destroyed, occluded site will soon form and restrict the diffusion of the oxygen into the pit. Chloride dominates the anion migration into the pit owing to its high mobility and concentration compared to the other anions [35-37]. Localized anode will form in the pit and provide electrons to the surrounding area. The high galvanic current will cause high dissolution rate of the anode and the oxygen on the steel surface will soon be consulted, leading to the corrosion processes controlled by the oxygen diffusion process [38-40].

Through the electrochemical test, it can be found that sulfate ions will destroy the passive film and cause the increase of the corrosion rate. However, sulfate ions are less aggressive compared to chloride ions and sulfate ions will soon absorb on the steel surface, leading to the repair effect of the passive film. Same phenomenon was found in Shaheen's [41] test that the passive zone of the steel is more in the conjoint presence of both chloride-sulfate ions as compared to the presence of only chloride ions. It also implies that sulfate ions had a migrate effect for the reducing of passivity range of the rebar due to the introduction of chloride ions. The rise of the OCP and the decrease of the corrosion rate are good certifications for the absorb effect of sulfate ions on the steel surface, leading to the prevention of the metal dissolution. The corrosion pattern of the electrode in the only sulfate contained solution is more close to average corrosion as shown in Fig. 6c.

In the solution contained with both sulfate ions and chloride ions, the passive film will be damaged immediately due to aggressive ions. Because competitive adsorption exists between the two kinds of ions, sulfate ions are more easily to absorb on the steel surface and prevent chloride ions to reach the steel [42]. Thus, the corrosion behavior is slighter than that in only chloride contained solution and close to the behavior in only sulfate contained solution. The inhibition effect of sulfate ions for the occluded pitting corrosion is also studied for the other passive metals [43-45]. It is found that the concentration of the chloride ions become smaller in the passive film when sulfate ions are mixed in the solution [45]. The high mobility of the sulfate ions will suppress the inward growth of the chloride ions into the defects of the passive film. In the studies conducted by Na [46], the electrochemical noise frequency between the aluminum electrodes have a significant decrease with sulfate ions added into the chloride contained solution. It shows that the corrosion process of the metal in passive state can be well inhibited by the sulfate ions. However, due to the existence of chloride ions, pits can still propagate with a low expansion rate on the steel surface.

Through the WBE test, the corrosion process can be reflected more clearly. It can be found that the anodic area and cathodic area on WBE surface became scattered after it transferred to the chloride contained solution. The rapid transform of the anodic areas indicate a metastable pitting corrosion

process on the WBE surface [47]. During this period, the breakdown and recover of the passive film is stochastic occurring on WBE surface. Once a stable pit is formed, most of the surface area will become cathodic area and anodic area will only focus on a small region with a high corrosion rate. While, in the solution contained both sulfate ions and chloride ions, the anodic area is nearly stable in the 10 days test. The rise of the anodic galvanic current density at the initial period and the following decrease also reflected the broken of the passive film and the following absorption processes of the sulfate ions. In the previous studies [40, 48], it is found that sulfate ions can lead to the rise of the pitting corrosion potential for the passive metals compared to only chloride ions contained solutions. It indicates that sulfate ions can mitigate the pitting corrosion chance of the rebar in chloride ions contained pore solution. From the WBE test, this phenomenon can be further evaluated by the calculating of localized corrosion factor. The localized corrosion factor *LF* which used by Dong [49] in the study of localized corrosion is involved to further characterize the localized corrosion level. *LF* can be expressed as:

$$LF = \sqrt{\sum_{j=1}^{N_a} (I_{j,g}^a)^2 \Big/ \sum_{i=1}^{100-N_a} (I_{i,g}^c)^2} \times \frac{N_c}{N_a} \tag{5}$$

Where N_a, N_c are the total number of wire electrodes with anodic and cathodic current values, respectively. The sum of N_a and N_c are apparently the total number of wire electrodes in the WBE. $I_{j,g}^a$, $I_{i,g}^c$ are the galvanic values corresponding to the jth anodic and ith cathodic wire electrodes, respectively. When localized corrosion happens, the higher anodic density and lower cathodic density will lead to a higher *LF* value. Fig. 12 shows the calculated *LF* value with the WBE immersed in Solution 2, 3 and 4, respectively. The *LF* of the WBE in Solution 2 reached nearly 250 after 10 days test. However, the *LF* of the WBE in Solution 3 is close to zero which means nearly no localized corrosion occurred in this condition. Furthermore, the *LF* of the WBE in Solution 4 was between that in Solution 2 and 3. It can be found that sulfate ions indeed have an excellent inhibit effect for the localized corrosion behavior caused by the aggression of chloride ion. It further verifies that sulfate ions can hinder the incorporation of chloride ions into the passive film.
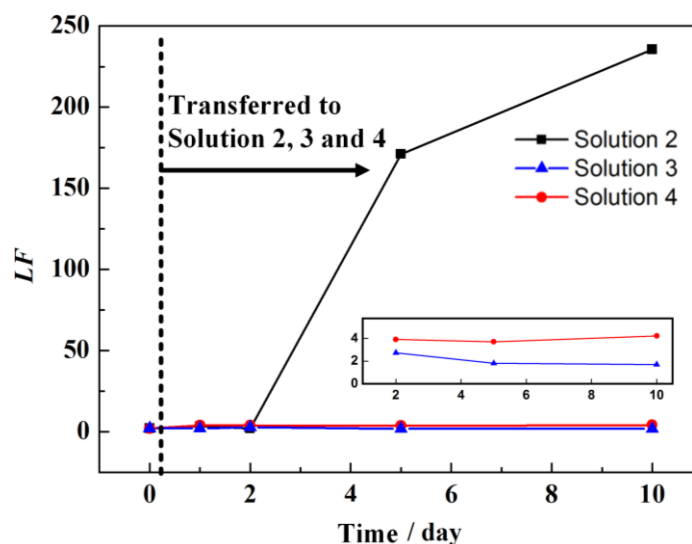

Figure 12. Time dependence of the LF with the WBE immersed in Solution 2, 3 and 4, respectively

4. CONCLUSIONS

In the simulated concrete pore solution, chloride ions have an intense aggression effect for the passive film and will cause serious localized corrosion. The localized penetration rate can reach 1.3 mm/a in 3% NaCl contained pore solution and *LF* reached nearly 250 also indicates a high level of localized corrosion. Sulfate ions will also cause the damage of the passive film. However, due to the absorption effect, sulfate ions will attached on the steel surface and repair the passive film. The corrosion pattern in only sulfate ions contained solution is close to uniform corrosion with just a few tiny pits. Due to the competitive adsorption effect between the sulfate ions and chloride ions, the corrosion rate in the solution contained with 3% NaCl and 0.5% $NaSO_4$ is much smaller than that in only 3% NaCl contained solution. WBE test result shows that sulfate ions also have an excellent inhibition effect for the localized corrosion caused by the self-catalysis effect of chloride ions in the occlude pits.

References

1. A. Poursaee, *Concr. Res. Lett*. 1 (2010) 90.
2. Y. Chen, Z. M. Yang, H. M. Wang, *J Iron Steel Res Int*. 19 (2012) 48.
3. S.M. Abd El Haleem, E.E. Abd El Aal, S. Abd El Wanees, A. Diab, *Corros. Sci*. 52 (2010) 3875.
4. S.M. Abd El Haleem, S. Abd El Wanees, E.E. Abd El Aal, A. Diab, *Corros. Sci*. 52 (2010) 292.
5. V. Bouteiller, C. Cremona, V. Baroghel-Bouny, A. Maloula, *Cement Concr. Res*. 42 (2012) 456.
6. Z. H. Dong, W. Shi, X. P. Guo, Corros. Sci. 53 (2011) 1322.
7. Y. Li, H. Zhang, X. Wang, Ji Li, F. Wang, *Corros. Sci*. 53 (2011) 4044.
8. X. Shi, N. Xie, K. Fortune, J. Gong, *Constr. Build. Mater*. 30 (2012), 125.
9. R. Vedalakshmi, N. Palaniswamy, *Mag Concrete Res*. 62 (2010) 177.
10. M. Ormellese, M. Berra, F. Bolzoni, T. Pastore, *Cement Concrete Res*. 36 (2006), 536.
11. J.J. Shi, W. Sun, *Cement and Concrete Composites*. 45 (2014) 166.
12. F.Xu, J. Duan, C. Lin, B. Hou, *J. Iron Steel Res. Int*. 22 (2015) 715.
13. M. Behpour, N. Mohammadi, E. Alian, *J. Iron Steel Res. Int*. 21 (2014) 121.
14. H. L. Cheng, H. Wang, N. B. Huang, *J. Iron Steel Res. Int.* 21 (2014), 444.
15. N. Naing Aung, Y. Tan, *Corros Sci*. 46 (2004) 3057.
16. F. Varela, M.Y.J. Tan, M. Forsyth, *ECS Electrochemistry Letters*. 4 (2014) C1.
17. Y. Tan, Corros Sci. 53 (2011) 1145.
18. W. Shi, Z.H. Dong, D.J. Kong, X.P. Guo, *Cement Concrete Res*. 48 (2013) 25.
19. Z.H. Dong, W. Shi, G.A. Zhang, X.P. Guo, *Electrochim. Acta*. 56 (2011) 5890.
20. Z.H. Dong, W. Shi, H.M. Ruan, G.A. Zhang, *Corros.Sci*. 53 (2011) 2978.
21. K. Premlall, J.H. Potgieter, S. Sanja, *Anti-Corros Method M*. 58 (2011) 267.
22. S.M. Abd El Haleem, S. Abd El Wanees, A. Bahgat, *Corros Sci*. 75 (2013) 1.
23. O. S. B. AL-Amoudi, Rasdeeduzzafar, M. Maslehuddin, S. N. Abduljauwad, *Concrete and Aggregates,* 16 (1994) 3.
24. O. S. B. Al-Amoudi, *Building & Environment*, 33 (1998) 53.
25. A. J. A1-Tayyib, S. K. Somuah, J. K. Boah, P. Leblanc, A. I. AI-Mana, *Cement Concrete Res*. 18 (1988) 774.
26. J. Soltis, *Corros Sci*. 90 (2015) 5.
27. C. Alonso, M. Castellote, C. Andrade, *Electrochim. Acta*. 47 (2002) 3469.
28. H. Yu, K.K. Chiang, L. Yang, *Constr Build Mater*. 26 (2012) 723.
29. Y.Z. Xu, Y. Huang, L. Ying, B. Li, X.N. Wang, *Acata Metall Sin*. 52 (2016) 320.

30. Y. Zou, J. Wang, Y. Y. Zheng, *Corros Sci.* 53 (2011) 208.
31. N.N. Aung, Y. J. Tan, *Mater Corros*. 57 (2006) 555.
32. W. Shi, Z.H. Dong, D.J. Kong, X.P. Guo, *Cement Concrete Res*. 48 (2013) 25.
33. C.Q. Ren, J.B. Chen, L.D. Pu, L. Liu, Y. Pan, J.Y. Hu, T. Shi, *Int. J. Electrochem. Sci.* 10 (2015) 8210.
34. J. Z. Liu, D. Zhao, J. S. Cai, L. Shi, J. P. Liu, *Int. J. Electrochem. Sci*. 11 (2016) 1135.
35. J. Soltis, *Corros Sci.* 90 (2015) 5.
36. Y.Z. Xu, L.J. Yang, L.M. He, Y. Huang, X.N. Wang, Corros. *Eng. Sci. Tech.* http://dx.doi.org/10.1080/1478422X.2016.1173313
37. Y.F. Cheng, J.L. Luo, *British Corros*. J. 35 (2013) 125.
38. Robert G. Kelly. Chemistry Electrochemical Techniques in Corrosion Science and Engineering, New York: Crc Press, 2003.
39. L. Bertolini, B. Elsener, P. Pedeferri, E. Radaelli, R. Polder, WILEY-VCH Verlag GmbH & Co. KGaA, Weinheim, 2013.
40. H. W. Song, H. J. Kim, V. Saraswathy, T. H. Kim, *Int. J. Electrochem. Sci.* 2 (2007) 341.
41. F. Shaheen, B. Pradhan, *Constr. Build. Mater*. 101 (2015) 99.
42. S.I. Pyun, S.M. Moon, S.H. Ahn, S.S. Kim, *Corros. Sci*. 41 (1999) 653.
43. W.J. Lee, S.I. Pyun, *Electrochim. Acta* 44 (1999) 4041.
44. W.J. Lee, S.I. Pyun, *Electrochim. Acta* 45 (2000) 1901.
45. K.H. Na, S.I. Pyun, *J. Solid State Electr*. 9 (2005) 639.
46. K.H. Na, S.I. Pyun, *J. Electroanal. Chem*. 596 (2006) 7.
47. Z.H. Dong, W. Shi, X.P. Guo, *Corros Sci*. 53 (2011) 1322.
48. A. Anderko, N. Sridhar, D. S. Dunn, *Corros Sci.* 46 (2004) 1583.
49. Z.H. Dong, W. Shi, X.P. Guo, *Acta Phys-Chim Sin*.27 (2011) 127.